INFLUENCE OF A RESIDUAL SURFACE STRESS FIELD NEAR THE CRACK TIP ON CRACK PROPAGATION

E. Welsch, D. Eifler, B. Scholtes and E. Macherauch*

Crack growth experiments using constant amplitude as well as overload tests have been performed with RCT-specimens of quenched and tempered SAE 4140. The stress distributions near the crack tip of loaded and unloaded specimens were determined by X-ray diffraction as a function of the crack length. Characteristic results are presented. The relationship between overload, residual stress fields and the crack propagation rate is discussed.

INTRODUCTION

In cyclic constant amplitude loading tests the fatigue crack growth rate can be described quantitatively in terms of the cyclic stress intensity range. During cycling of cracked parts with variable amplitudes and different mean stresses, accelerations as well as retardations of fatigue crack growth rate have been observed. In this important case no simple models are available for lifetime assessments because of the multiplicity of influencing parameters. Crack propagation is, among others, influenced by the residual stress field of a growing crack which is a consequence of local inhomogeneous plastic deformations in the crack tip region. Actually residual stress effects, although mostly not exactly known, are implicitly included in all quantitative descriptions of crack propagation. Up to now, however, no systematic investigations exist about the residual stress states of fatigue cracked specimens and their changes with crack propagation during cyclic loading. Also, no quantitative data exist about the actual total stresses in the crack tip area as a consequence of superpositions of fatigue induced residual stresses and loading stresses.

* Institut für Werkstoffkunde I, University of Karlsruhe, Kaiserstraße 12, D-7500 Karlsruhe, FRG

This paper describes the surface residual stress states and the total surface stresses near the crack tip of Round Compact Tension, RCT-specimens (Feddern and Macherauch [1]) which have been fatigued in constant amplitude as well as overloading tests.

STATE OF KNOWLEDGE

Experimental investigations about the residual or total stress fields near the crack tip of cracked specimens and parts are scarce. Quasistatic loaded centre cracked specimens of Ck 45 were measured (Hellwig and Macherauch [2-4]) and a good agreement was found between the experimentally determined loading and residual stresses and theoretical expectations. In addition, the residual and total stress distribution have been successfully modelled by finite element calculations (Schröder et al [5]). Also some experimental results concerning residual stresses near the crack tip of fatigue cracks exist. After applying specific loading conditions, the residual stress field around a fatigue crack tip and the plastic zone size were examined, including investigations about the variation of both quantities over the thickness of the cracked specimens (Schlosberg and Cohen [6]). Residual and loading stresses near the crack tip in both the ferrite and cementite phase of a tool steel were determined (Blumenauer and Zutkhoff [7]). Qualitatively similar stress distributions were found with significantly higher stresses in cementite than in ferrite. In other experiments, also residual stresses at the crack edges of fatigue cracked specimens have been observed indicating crack closure effects [3]. It was shown (Honda et al [8,9]) that the area with compressive residual stresses at the crack edges increases with decreasing stress amplitude during fully reversed loading. Further investigations revealed, that the area affected by compressive residual stresses in front of the crack increases with increasing stress intensity factor and decreases with yield strength of the material investigated ([5,9], Kunz et al [10]). The maximum compressive residual stress value, however, increases with yield strength. Finally, the influence of single or multiple overloads on the residual stress distributions in front of and around fatigue cracks have been studied. For example, residual stresses and total stresses in the ligament of tension-tension loaded plain carbon steels have been analysed (Allison [11]). The observed crack retardation effects after overloadings were considered as a consequence of the increase of the region with compressive residual stresses in front of the crack tip.

MATERIAL AND TEST CONDITIONS

The material used was a quenched and tempered SAE 4140 steel. In monotonic tensile tests with a strain rate $\dot{\varepsilon} = 3{,}47 \cdot 10^{-4}\ s^{-1}$ a 0.2 % proof stress $R_{p0,2} = 975\ N/mm^2$, a tensile strength $R_m = 1048\ N/mm^2$, a tensile elongation $A = 8{,}6\ \%$ and a reduction of area $Z = 57\ \%$ were measured. The crack growth experiments were performed

using RCT-specimens (see also ASTM E 647) with B = 10 mm, W = 45 mm, D = 60 mm and a_o = 13 mm). Both constant amplitude and overload tests were carried out using triangular loading cycles, as schematically shown in Fig. 1. In all cases the basic loading was at 10 Hz with a stress ratio $\chi = \sigma_{\ell 1}/\sigma_{u1} = 0.05$ and a stress range $\Delta\sigma_1 = 21$ N/mm^2. In the overload tests after reaching a crack length of 16 mm always 10 overload cycles were applied at 0.1 Hz with $\Delta\sigma_2 = 37$ or $\Delta\sigma_2 = 63$ N/mm^2 resp. which yield overload ratios $\lambda = 1.75$ and $\lambda = 3.0$ resp. Further cycling up to fracture was completed again at the basic stress range $\Delta\sigma_1$. The corresponding stress intensity ranges ΔK were calculated as

$$\Delta K = \frac{\Delta F}{BW} \cdot Y \cdot \sqrt{a} \qquad \text{where:} \quad \Delta\sigma = \frac{\Delta F}{BW} \tag{1}$$

with ΔF loading range and

$$Y = 29.6 - 162\left(\frac{a}{w}\right) + 492.6\left(\frac{a}{w}\right)^2 - 663.4\left(\frac{a}{w}\right)^3 + 405.6\left(\frac{a}{w}\right)^4 \tag{2}$$

geometry factor [1].

Surface residual and total stress components perpendicular to the ligament of the specimens were determined by X-ray diffraction. The $\sin^2\psi$-method (Macherauch and Müller [12]) was applied using CrKα-radiation with a computerized ψ-diffractometer of the Karlsruhe-type. A special cardanic specimen holder improved the measuring conditions. To adjust the position of the primary X-ray beam with an accuracy of about 0,05 mm, a light optical system was employed. The irradiated surface area was circular in shape with a diameter of 0.23 mm. For the determination of each stress component, {211}-lattice strains of the ferrite of the material were measured in 11 directions ψ with $\Delta\psi = 9°$ in the range $-45° \leq \psi \leq +45°$. ψ denotes the angle between the normal to the surface of the specimen and the measured directions, which always coincided with the normals of {211}-planes of special oriented ferrite grains. Stress calculations were made without taking into account the influence of elastic anisotropy. Consequently, Young's modulus E = 210000 N/mm^2 and Poisson's ratio $\nu = 0.28$ were used.

EXPERIMENTAL RESULTS

Fig. 2 shows for constant amplitude loading with $\chi = 0.05$ and $\Delta\sigma_1 = 21$ N/mm^2 the fatigue crack growth rate as a function of the crack length. A nearly linear relationship exists up to a crack length of 28.5 mm. After $11.8 \cdot 10^4$ cycles the specimen fails by unstable crack propagation. Residual stress distributions in the crack tip region after reaching crack lengths of 16 and 21 mm resp. are plotted in Fig. 3. In both cases similar residual stress distributions are observed. Always at the crack tip, maximum compressive residual stresses occur accompanied by a very steep stress gradient towards regions in front of the crack tip. In certain distances from the

crack tip maximum tensile residual stresses occur. On the other hand, the compressive residual stresses decrease slowly from maximum values at the crack tip to zero along the edges of the crack. Evidently, the maximum compressive residual stresses at the crack tip as well as the extension of the area affected by compressive residual stresses at the crack edges increase with increasing crack length. However, no pronounced influences of the actual crack length on the tensile residual stress distribution in front of the crack tip can be seen.

Fig. 4 summarizes for the same crack lengths as in Fig. 3 the experimentally determined total stress distributions occurring if the residual stressed specimens are statically loaded with the maximum stress of the loading cycles applied during the crack growth test. Independent of the crack length maximum tensile stresses always occur at the crack tip. The stress values decrease rapidly in front of the crack with increasing distances from the crack tip. The maximum values increase from 510 to 780 N/mm^2 if the crack grows from 16 to 21 mm.

Fig. 5 shows the fatigue crack growth rate as a function of the crack length of an overload experiment applying 10 overloads with $\Delta\sigma_2$ = 37 N/mm^2 (overload ratio λ = 1.75). Immediately after overloading an acceleration of the crack propagation is observed followed by a pronounced retardation. After reaching a crack length of about 17 mm the fatigue crack growth rate corresponds again to that observed at constant amplitude loading (Fig. 2).

Fig. 6 shows at crack lengths of 16 mm - this is the crack length immediately after overloading - and 16,5 mm (dotted lines in Fig. 5), the residual stress distributions at the crack tip. As can be seen, quite different results occur compared to observations at constant amplitude loading in Fig. 3. The maximum compressive residual stresses near the crack tip are higher and the stress gradients are still more pronounced. Furthermore, the residual stress distribution along the crack edges have remarkably changed. It is interesting to note that - in contrast to the upper picture in Fig. 3 - at a crack length of 16 mm behind the crack tip no and at 16.5 mm only in a very small area compressive residual stresses can be detected.

Applying statically the maximum stress of the basic loading cycles after reaching crack lengths of 16 and 16.5 mm resp. the total stress distributions in Fig. 7 are measured. Immediately after overloading the maximum tensile stresses at the crack tip are markedly reduced compared with those occurring at this crack length in specimens loaded with constant amplitudes (see upper part of Fig. 4). The maximum tensile stresses do not occur exactly at the crack tip but about 1 mm in front of it. After further growth of the crack from 16 to 16.5 mm - as shown in the lower part of Fig. 7 - a continuously decreasing total stress distribution is observed

comparable with the distributions in Fig. 4.

If under the same conditions as before at a crack length of 16 mm the overload ratio is increased from $\lambda = 1.75$ to $\lambda = 3.0$ more pronounced effects are observed. As can be seen from the upper part of Fig. 8, crack arrest occurs. Near the crack tip (middle part of Fig. 8) compressive residual stresses with a maximum value of about -750 N/mm^2 are measured. Static loading with the maximum stress of the basic loading cycles causes about 0.5 mm in front of the crack a total stress value of about -170 N/mm^2 (lower part of Fig. 8). After further crack propagation up to 16.7 mm, where the crack arrests, the distribution of the total surface stresses in front of the crack tip are only slightly changed.

DISCUSSION

The experimental results presented show that a clear correlation exists between loading conditions, crack growth rates and surface residual stress fields near the crack tip of fatigued RCT-specimens. In the case of constant amplitude loading, the observed residual stress distributions (Fig. 3) with compressive residual stresses along the crack edges and a maximum near the crack tip are explainable as a consequence of inhomogeneous plastic deformations in front of the crack tip and crack closure effects during the individual loading cycles. The very narrow zone of compressive residual stresses in front of the crack with a steep stress gradient is a consequence of the materials state. According to Irwin (Irwin and McClintock [13]) the quenched and tempered material should reveal at $a = 16$ mm and $\Delta\sigma = 21$ N/mm^2 a plastic zone radius of only about 0.32 mm. In Fig. 9 the residual stresses in front of the crack tip of a specimen after loading with $\Delta\sigma = 21$ N/mm^2 up to a crack length of 16 mm, are compared with the residual stress distribution estimated with the simple Rice-model (Rice [14]) assuming elastic plastic materials behaviour. At the best only a qualitative agreement can be stated. As a consequence of the small plastic zone size and the corresponding steep stress gradients the X-ray method used always determines averaged values of the real existing stresses [5]. As expected, in the area of maximum compressive residual stresses in front of the crack tip and in the area of maximum tensile residual stresses the measured values are smaller than the estimated ones. Besides the simplifications of the theoretical model further assessments of these observations have also to consider the consequences of e.g. cyclic softening, strain hardening, Bauschinger effect, lower yield strength of the surface crystallites and crack closure effects on the resultant residual stress field.

According to the results in Fig. 3 both the residual stress affected regions around the crack tip and the amount of maximum compressive residual stress increase with growing fatigue crack length and plastic zone size. In addition, with increasing crack

length a decreasing relative crack closure zone is observed. The magnitudes of the total stresses in front of the crack (Fig. 4) which represent the superpositions of loading and residual stresses, are shifted to higher values with increasing crack length. In all cases the tensile stresses reach highest values at the crack tip and decrease with increasing distance from the crack. However, no remarkable discontinuity due to the residual stresses can be noticed.

In this connection, a comparison between theoretically estimated and real existing surface stress distributions seems to be interesting. In Fig. 10 the calculated loading stress distribution of a residual stress free specimen with a crack length of 21 mm is compared with the measured total stress distribution already shown in the lower part of Fig. 4 of an equally loaded specimen bearing residual stresses due to crack growth. At the crack tip the yield strength of the material is not reached by the experimental values. The difference of about 150 N/mm^2 between the measured and the calculated values at greater distances from the crack tip is not understood. Obviously, a simple linear superposition of surface residual and loading stresses does not occur.

The theoretically estimated radius of the plastic zones expected after overloading applying the overload ratios $\lambda = 1.75$ and $\lambda = 3.0$ are 0.93 and 2.66 mm resp. The experimentally observed values of 0.8 and 3.8 mm agree quite well with these estimations, taking the simplifications of the theory into account.

In Fig. 11 the measured residual stress distribution after overloading a single step loaded specimen at a crack length of 16 mm with an overload ratio $\lambda = 3.0$ is compared with the calculated residual stress distribution according to the Rice-model. Again only a qualitatively satisfying agreement between measurement and calculation exists. As a consequence of the larger plastic zone in this case a more extended area in front of the crack tip bearing residual stresses equal to the yield stress is calculated than in Fig. 9. It is interesting to note that in front of the crack tip really no constant maximum compressive residual stresses are observed. The surface residual stresses reach maximum values in a certain distance from the crack tip and increase in magnitude with increasing overload ratio (see upper part of Fig. 6). Also the zone with compressive residual stresses grows with overload ratio and crack length. In all cases immediately after overloading the crack is opened and no compressive residual stresses can be measured at the crack edges.

The total stresses measured after overloading are considerably different to those measured in constant amplitude tests. In these cases the superposition of external stresses with the overload induced residual stress fields mostly do not lead to continuously decreasing stress values with increasing distance from the crack

tip. Immediately after overloading the maximum values of the tensile stresses at the crack tip are significantly lowered. As an example in Fig. 12 for $\lambda = 3$ and a = 16 mm the theoretical expected total stresses are compared with the measured values. It can be seen that the calculated total stress field resembles the observed one only very roughly. In particular the steep stress gradients and the maximum tensile and compressive stress values in front of the crack tip are not experimentally confirmed.

It is generally accepted that the cyclic stress intensity range

$$\Delta K = K_{max} - K_{min} \text{ for } K_{min} > 0 \tag{3}$$

and

$$\Delta K = K_{max} \text{ for } K_{min} \leq 0 \tag{4}$$

controls the propagation of fatigue cracks during constant amplitude loading. The influence of residual stresses on fatigue crack growth rate can quantitatively be taken into account by the residual stress intensity K^{RS} belonging to the particular crack shape and residual stress distribution. Consequently, the loading stress intensities K_{max}^{LS} and K_{min}^{LS} have to be corrected for the influence of residual stresses by calculating an effective stress intensity range

$$\Delta K_{eff} = K_{eff,max} - K_{eff,min} \tag{5}$$

with

$$K_{eff,max} = K_{max}^{LS} + K^{RS} \tag{6}$$

and

$$K_{eff,min} = K_{min}^{LS} + K^{RS} \tag{7}$$

In the case of $K_{eff,min} > 0$, only a small influence of residual stresses on the fatigue crack growth rate is expected as a consequence of the changing of the effective stress ratio

$$\chi_{eff} = \frac{K_{min}^{LS} + K^{RS}}{K_{max}^{LS} + K^{RS}} \tag{8}$$

However, in the case of $K_{eff,min} \leq 0$, distinct residual stress effects on the fatigue crack propagation have to be expected (Macherauch [15]).

As a consequence of the very low total stresses in front of the crack tip, in loaded specimens immediately after overloading the effective stress intensity range of the basic loading cycles following the overloads is drastically diminished. As a consequence of the local reduction of the effective stress intensity range, also the fatigue crack growth rate is reduced. This reduction increases with increasing overload ratio . Obviously, in the case of $\lambda = 3$ the effective stress intensity range after overloading is

about ΔK_o since crack arrest is observed. Also the development of the plastic zone size of the propagating fatigue crack after overloading displays the influence of the residual stress field. This is demonstrated in Fig. 13. In the upper part, the increasing plastic zone size with increasing crack length and the plastic zone due to overloading can be recognized. The lower part of the figure shows the very small plastic zone size during crack propagation immediately after overloading, increasing with further crack growth.

Another factor contributing to crack growth retardation is crack closure due to compressive residual stresses acting at the crack edges. According to Fig. 6 after overloading these residual stresses increase with increasing crack length. Consequently, the effective stress intensity range is decreased and higher external stresses are necessary to open the crack.

Altogether there is little doubt that the observed crack growth retardations and arrest effects are mainly due to the residual stress field which is produced as a consequence of the overloadings.

REFERENCES

[1] Feddern, G. and Macherauch, E., Z. Metallkunde 64, 1973, pp. 882-884.

[2] Hellwig, G. and Macherauch, E., Z. Metallkunde 65, 1974, pp. 75-79.

[3] Hellwig, G. and Macherauch, E., Z. Metallkunde 65, 1974, pp. 496-500.

[4] Hellwig, G. and Macherauch, E., Z. Werkstofftechnik 5, 1974, pp. 341-348.

[5] Schröder, R., Wolfstieg, U. and Macherauch, E., "Eigenspannungen", Deutsche Gesellschaft für Metallkunde, Oberursel, 1979, pp. 107-120.

[6] Schlosberg, W.H. and Cohen, J.B., Metallurgical Transactions 13A, 1982, pp. 1987-1995.

[7] Blumenauer, H. and Zutkhoff, B., Problemy Prochnosti 3, 1981, pp. 18-20.

[8] Honda, K., Hosokawa, T., Sarai, T. and Okamoto, K., J. Soc. Materials Science Jap. 31, 1982, pp. 8-12.

[9] Honda, K., Torii, T. and Toi, N., Zairyo, Tokyo, 33, 1984, pp. 209-215.

[10] Kunz, L., Knesl, Z. and Lukas, P., Fatigue of Engineering Materials and Structures 2, 1979, pp. 279-287.

[11] Allison, J.E., ASTM STP 677, 1979.

[12] Macherauch, E. and Müller, P., Z. angew. Physik, 13, 1961, pp. 305-312.

[13] Irwin, G.R. and McClintock, R., ASTM STP 381, 1965.

[14] Rice, G.R., ASTM STP 415, 1967.

[15] Macherauch, E., "Residual Stresses", Martinus Nijhoff Publishers, The Hague, Boston, Lancaster, 1984, pp. 157-192.

SYMBOLS USED

a:	crack length
B:	specimen thickness
D:	specimen diameter
da/dx:	crack growth rate
E:	Young's modulus
K_{min}:	minimum stress intensity
K_{max}:	maximum stress intensity
$K_{eff,min}$:	minimum effective stress intensity
$K_{eff,max}$:	maximum effective stress intensity
ΔK:	stress intensity range
ΔK_{eff}:	effective stress intensity range
W:	specimen width
Y:	geometry factor
χ:	stress ratio
χ_{eff}:	effective stress ratio
λ:	overload ratio
σ_{l1}:	minimum stress of the basic stress range
σ_{u1}:	maximum stress of the basic stress range
σ_{l2}:	minimum stress of the overload stress range
σ_{u2}:	maximum stress of the overload stress range
$\Delta\sigma_1$:	basic stress range
$\Delta\sigma_2$:	overload stress range
σ^{RS}:	residual stress
σ^{TS}:	total stress

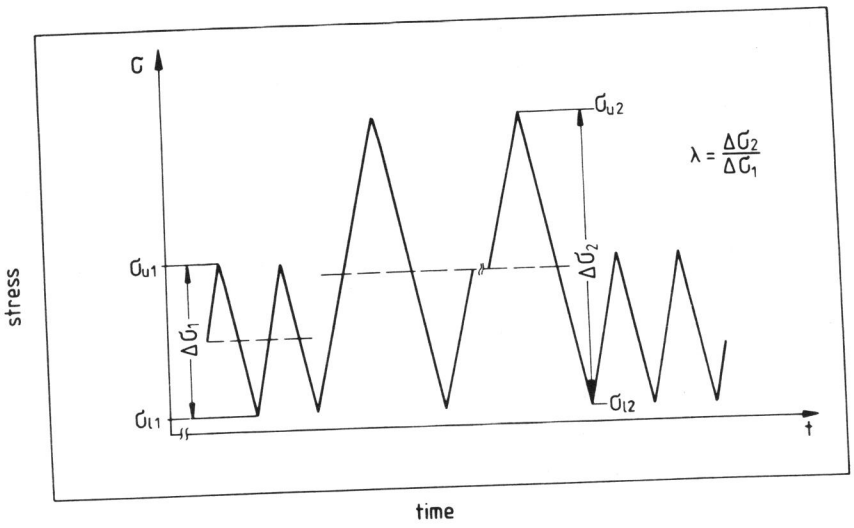

Figure 1 Schematical loading sequence diagram

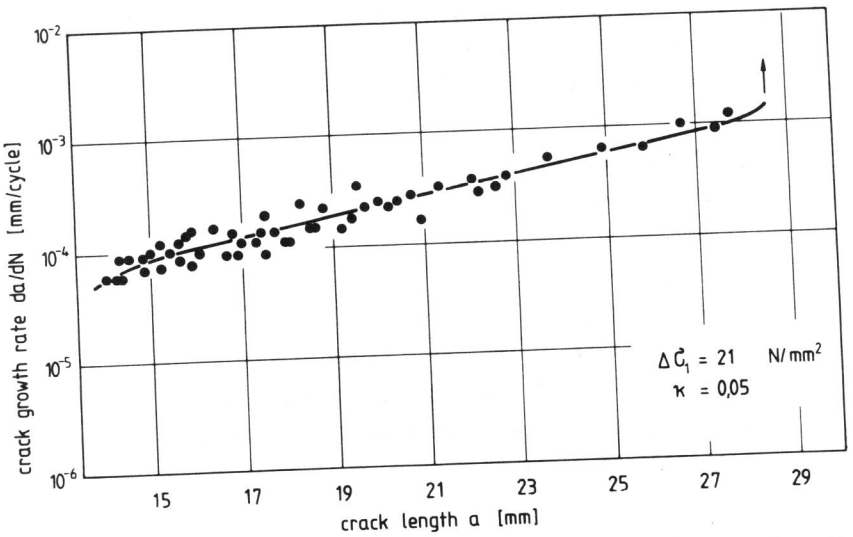

Figure 2 Fatigue crack growth rate as a function of crack length for constant amplitude loading

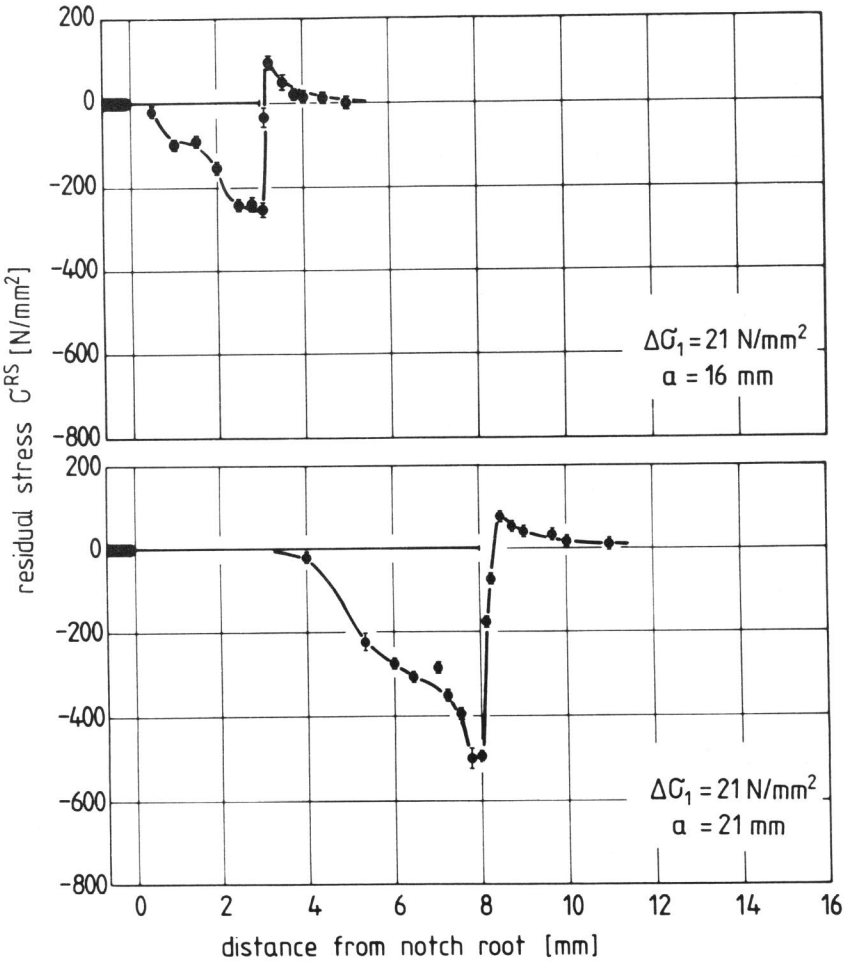

Figure 3 Residual stresses σ^{RS} in the crack tip region for different crack lengths

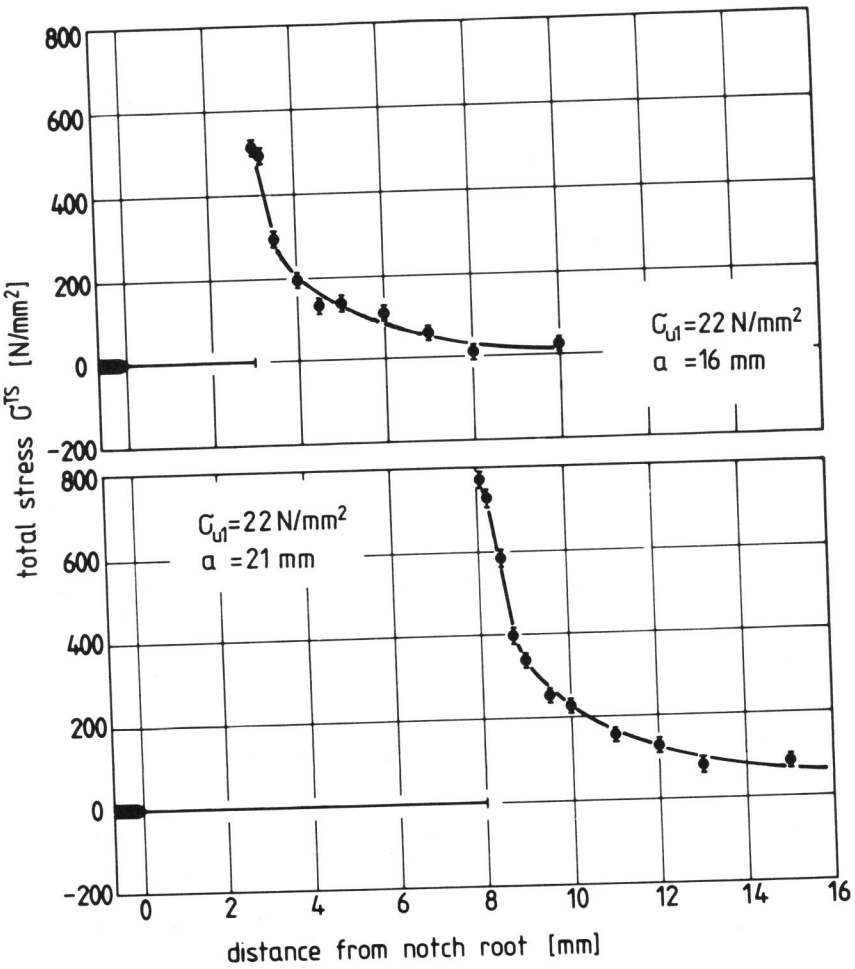

Figure 4 Total stresses σ^{TS} in the crack tip region for different crack lengths

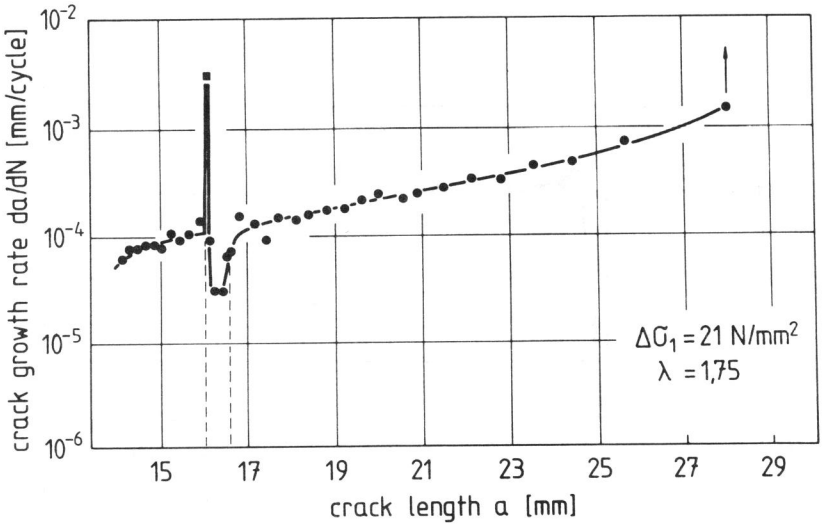

Figure 5 Fatigue crack growth rate as a function of crack length for an overloading test with $\lambda = 1.75$

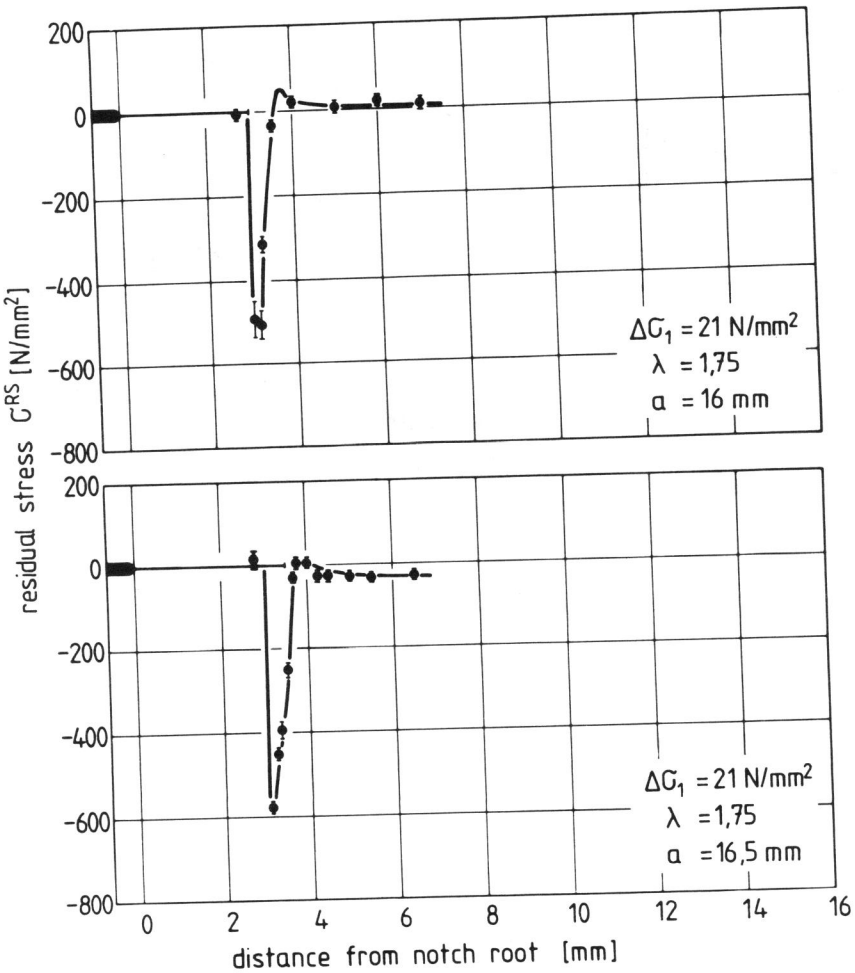

Figure 6 Residual stresses σ^{RS} in the crack tip region for crack lengths of 16 and 16.5 mm after an overloading test with λ = 1.75

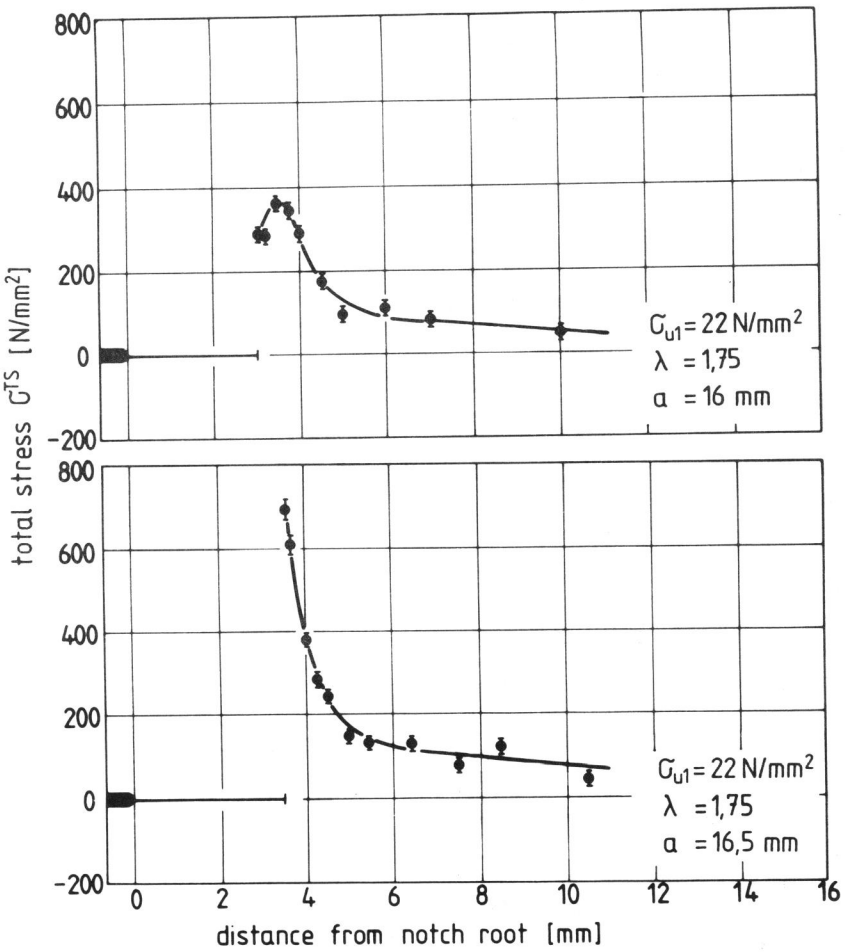

Figure 7 Total stresses σ^{TS} in the crack tip region for crack lengths of 16 and 16.5 mm after an overloading test with λ = 1.75

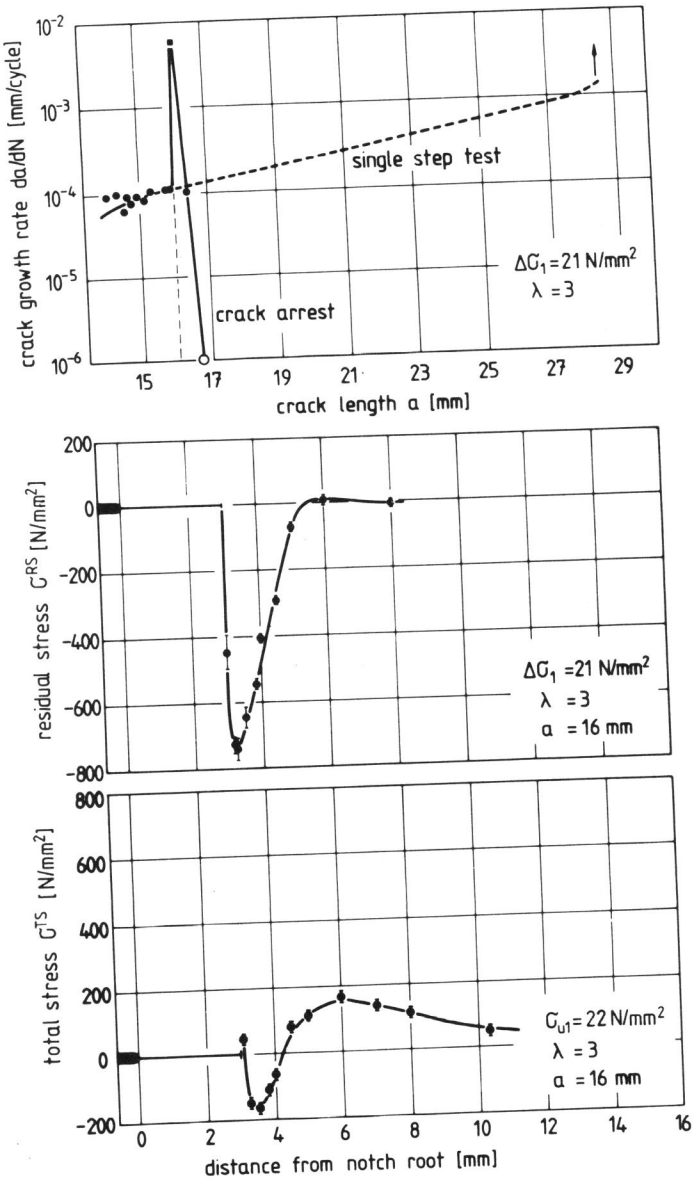

Figure 8 Fatigue crack growth rate, residual and total stress distribution after an overloading test with $\lambda = 3$

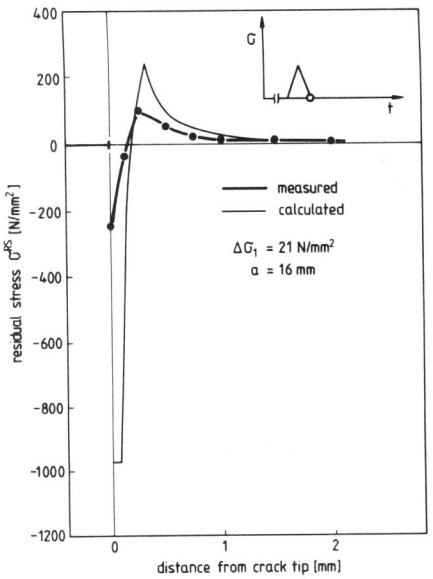

Figure 9 Measured and calculated stresses σ^{RS} (λ = 1)

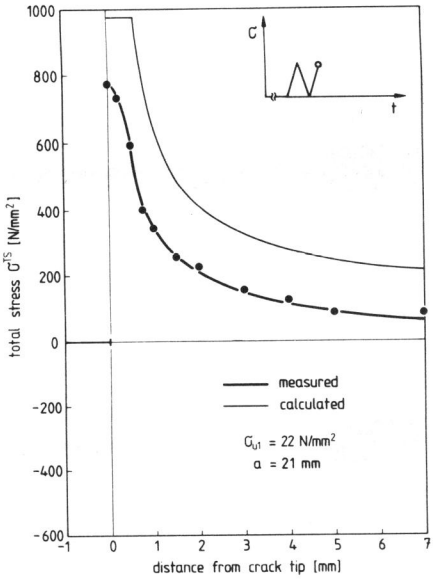

Figure 10 Measured and calculated stresses σ^{TS} (λ = 1)

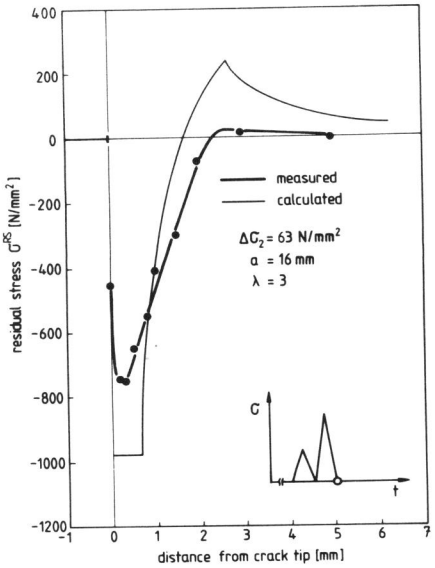

Figure 11 Measured and calculated stresses σ^{RS} (λ = 3)

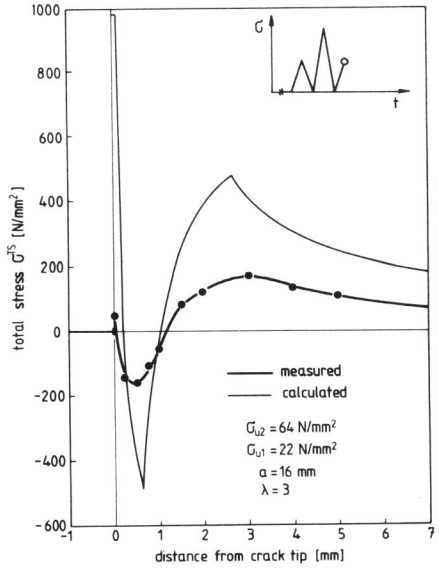

Figure 12 Measured and calculated stresses σ^{TS} (λ = 3)

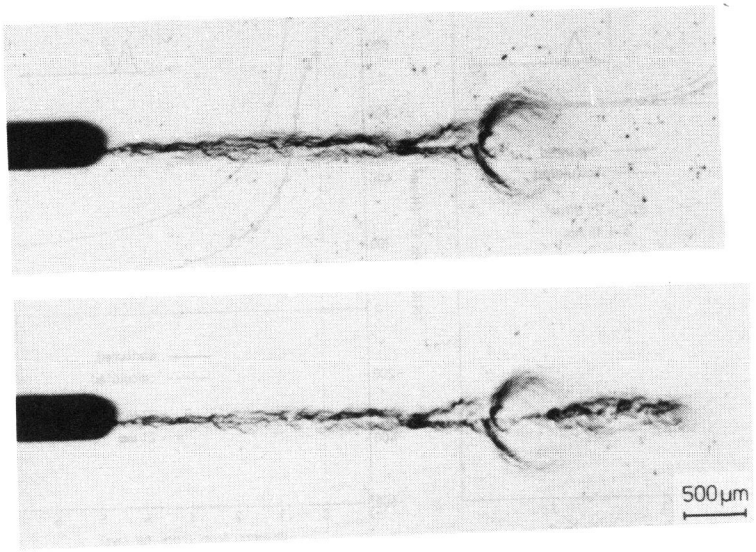

Figure 13 Development of the plastic zone